



# Amperometric sensing of nitrite at nanomolar concentrations by using carboxylated multiwalled carbon nanotubes modified with titanium nitride nanoparticles

Muthaiah Annalakshmi<sup>1</sup> · Paramasivam Balasubramanian<sup>1</sup> · Shen-Ming Chen<sup>1</sup>  · Tse-Wei Chen<sup>1,2</sup>

Received: 14 September 2018 / Accepted: 29 November 2018 / Published online: 10 December 2018  
© Springer-Verlag GmbH Austria, part of Springer Nature 2018

## Abstract

A glassy carbon electrode (GCE) was modified with a nanocomposite prepared from carboxylated multiwalled carbon nanotubes (c-MWCNT) and titanium nitride (TiN) nanoparticles to obtain a sensor for nitrite. The nanocomposite was characterized by transmission electron microscopy, elemental mapping, X-ray diffraction, and Raman spectroscopy. Electrochemical studies results show the modified GCE to possess a low electrochemical resistance ( $R_{ct} = 7 \Omega$ ) and a large electroactive surface ( $A = 0.112 \text{ cm}^2$ ). The heterogeneous electron transfer rate ( $k_s$ ) is found to be  $1.26 \times 10^{-2} \text{ cm s}^{-1}$ . Due to the excellent synergistic effect of c-MWCNT and TiN, the GCE displays an excellent performance in terms of nitrite sensing. At a typical working voltage of +0.8 V (vs. Ag/AgCl), the limit of detection (LOD) is as low as 4 nM, and the useful analytical range extends from 6 nM to 950  $\mu\text{M}$ . This is much better than the LODs of previously reported nitrite sensors. The sensor is fast (response time 4 s), selective, and long-term stable. It was applied to the determination of nitrite in spiked water and meat samples and gave good recoveries.

**Keywords** Inorganic pollutants · Methemoglobinemia · Heterogeneous electron transfer rate · Low impedance · Electrochemical sensor

## Introduction

Nitrite ( $\text{NO}_2^-$ ) is one of the well-known inorganic pollutants hazardous to environment and living organisms [1]. Nitrites are used in various fields such as food industries (additives or preservatives), corrosion inhibitors, fertilizers and as a blood pressure lowering agent in medicine [2]. In the human body, the excess level of nitrite can irreversibly react with hemoglobin to produce

methemoglobin, which decrease the oxygen transport capability of blood [3]. Nitrite ions easily react with amines and proteins of living organisms, converting them to carcinogenic N-nitrosamines, which probably induce the Blue baby syndrome and cancer [4]. The acceptable level of nitrite in drinking water is  $50 \text{ mg L}^{-1}$ , according to World Health Organization [5]. When untreated and overdosed, ultimately outcomes in death owing to the oxygen deficiency [6]. Therefore, the need to develop reliable quantitative methods for determination of the low-level nitrite is important for environmental protection as well as human health. Number of analytical methods for the nitrite detection includes UV/Vis, fluorimetry, chromatographic, capillary electrophoretic, spectrophotometric, electrochemiluminescence, Infra-Red, Raman, and electrochemical methods [7]. Amongst, electrochemical methods have significant advantages including rapidity, low-cost, safer, high selectivity and sensitivity [8–10]. However, the oxidation of nitrate at bare electrode occurring at a high voltage, can interfere with the oxidizable species [11]. Hence, the development of modified electrode using a desirable electrode material to detect the nitrite ions at lower overpotential with high sensitivity is highly necessary.

**Electronic supplementary material** The online version of this article (<https://doi.org/10.1007/s00604-018-3136-4>) contains supplementary material, which is available to authorized users.

✉ Shen-Ming Chen  
smchen78@ms15.hinet.net

<sup>1</sup> Department of Chemical Engineering and Biotechnology, National Taipei University of Technology, Taipei 106, Taiwan, Republic of China

<sup>2</sup> Research and Development Center for Smart Textile Technology, National Taipei University of Technology, No.1, Section 3, Zhongxiao East Road, Taipei 106, Taiwan, Republic of China

Carbon, metal- and metal oxide-based nanomaterials have been reported as an electrode modifier to improve the electron transfer rate between the electroactive analytes and the surface of electrodes [12]. Amongst, carbon nanotubes have served as a perfect nanomaterial for sensing applications owing to its peculiar physicochemical properties such as special tube-like structure, large surface area, high thermal, and electrical conductivity [13, 14]. Because of the electrochemical stability of CNTs attributed to the presence of reactive groups on their surface, they can promote the electron transfer rate [15]. Excellent electrochemical conductivity of CNTs can influence the overpotential of the target analyte, and enhance the sensitivity. Metal nitrides are becoming promising materials for the electrochemical and photochemical applications due to the large surface area and chemical stability [16]. TiN upholds a number of unique properties such as high electrical conductivity, low resistivity, and high stability [17, 18]. TiN serves as a good corrosion inhibitor owing to the presence of triple covalent bond between nitrogen and titanium, it was reported as an efficient nanomaterial for various applications such as dye sensitized solar cells [19], catalysts [20] and super capacitors [21]. However, the previous publications confirmed that the TiN was slightly instable in aqueous electrolyte solution because of irreversible electrochemical oxidation [22]. To overcome this drawback, TiN composite has been fabricated with highly conductive carbon-based nanomaterials. Thus, it enhances the electrochemical performance and stability of the resultant nanocomposite [23].

We have synthesized the TiN nanoparticles decorated c-MWCNT by a two-step method. The fabricated c-MWCNT/TiN electrode was utilized as an electrochemical sensor for the detection of nitrite. The important electrochemical parameters such as impedance ( $R_{ct}$ ), electroactive surface area ( $A$ ), number of transferred electron ( $n$ ), and heterogeneous electron transfer rate ( $k_s$ ) for nitrite oxidation were discussed. The sensor has a very low detection limit, wide linear range, rapid response, and good selectivity for the detection of nitrite. The practical applicability of the sensor was evaluated using real water samples.

## Experimental

### Material and methods

Titanium nitrate ( $Ti(NO_3)_4 \cdot 4H_2O$ ), carboxylated multiwalled carbon nanotube (c-MWCNT), sodium nitrite ( $NaNO_2$ ), disodium hydrogen phosphate ( $Na_2HPO_4$ ), and sodium dihydrogen phosphate ( $NaH_2PO_4$ ) were purchased from sigma Aldrich (<https://www.sigmaldrich.com/catalog/product>). All chemicals and reagents were of analytical grade and used

as received. CHI 900 work station (CH Instruments Company, made in the U.S.A). was used perform all the electrochemical experiments (cyclic voltammetry and amperometry). The X-ray diffraction data were collected by using a XPERT-PRO diffractometer equipped with Cu  $K\alpha$  radiation ( $k = 1.54 \text{ \AA}$ ). The morphological structure of c-MWCNT-TiN was investigated by transmission electron microscopy (TEM) on a TECNAI  $G^2$  with an accelerating voltage of 200 kV. A Clean pH meter (pH 500) with a combined pH glass electrode was used measure the pH. Electrochemical impedance measurements were taken from an IM6ex (ZAHNER elektrik) at a potential of 0.2 V (AC potential: 5 mV) within a frequency range of 0.01 to 100 kHz. The conventional three electrode system was used for the electrochemical studies, the modified glassy carbon electrode, saturated silver/silver chloride (Ag/AgCl), and platinum wire were used as a working electrode (electrode area:  $0.07 \text{ cm}^2$ ), reference electrode and counter electrode, respectively.

### Synthesis of the c-MWCNT/TiN nanocomposite

The c-MWCNT/TiN nanocomposite were prepared via a two-step method. In order to prepare c-MWCNT/TiO<sub>2</sub> composite, 50 mg of c-MWCNT was dispersed in 50 mL DI water with the aid of ultrasonication. Afterwards, 100 mg  $Ti(NO_3)_4 \cdot 4H_2O$ , were added into the c-MWCNT dispersion and sonicated for 1 h. Then the mixture was refluxed for 6 h to coat the TiO<sub>2</sub> precursor on the surface of c-MWCNT. The resulting c-MWCNT-TiO<sub>2</sub> were collected and washed with DIW, dried at 80 °C. To prepare c-MWCNT-TiN nanocomposite, c-MWCNT-TiO<sub>2</sub> was located in a tubular furnace, annealed to 300 °C with a heating rate of 5 °C  $min^{-1}$  under a flowing gaseous  $NH_3$ . After completion of annealing, the furnace was allowed to cool down to room temperature naturally. Finally, the c-MWCNT-TiN nanocomposite was collected and used for further characterization.

### Preparation of the modified glassy carbon electrode

To fabricate the c-MWCNT/TiN/GCE, a glassy carbon electrode (GCE) was well polished with 0.05 mm alumina powder, carefully washed with deionized water (DIW) and acetone, until mirror-like surface. Then the GCE was ultrasonically cleaned with DIW: Ethanol (1:1) for 2 min, the electrode was washed with DIW and dried at room temperature. Lastly, 6  $\mu$ l of c-MWCNT/TiN dispersion ( $1 \text{ mg mL}^{-1}$ ) was dropped on the mirror-like GCE surface, allowed to drying at a hot air oven. Thus, prepared c-MWCNT/TiN modified GCE was used for further investigation.

## Results and discussion

### Choice of materials

Owing to the excellent electrical conductivity, large surface area, high stability of the c-MWCNT have been received enormous research interest in electrochemical sensor application [13]. The presence of triple covalent bond between titanium and nitrogen in TiN, it has been reported as an effective catalyst for electrochemical energy storage and conversion and catalysis applications [19–21]. However, the preparation of TiN nanoparticles supported c-MWCNT with facile and low temperature and its electrochemical sensor application is reported not yet. Therefore, we have synthesized the TiN nanoparticles decorated c-MWCNT nanocomposite at low temperature. The c-MWCNT/TiN nanocomposite is successfully employed as an excellent electrocatalyst for the detection of nitrite.

### Characterization of c-MWCNT/TiN nanocomposite

The morphology and structure of c-MWCNT/TiN nanocomposite were inspected by TEM. TEM images of c-MWCNT/TiN nanocomposite (Fig. 1a and b) displayed a number of TiN nanoparticles decorated on the surface of c-MWCNTs with a uniform dispersion. Energy dispersive X-ray spectroscopy (EDS) mapping was used to analyze the elements present and their distribution in c-MWCNT/TiN nanocomposite. As

shown in Fig. 1c (titanium) and d (nitrogen), the major EDS signals of titanium and nitrogen were derived from the identical area, representing the TiN formed as a nanoparticle, supported on the c-MWCNT surface. EDS mapping of carbon and oxygen are also shown in Fig. S1A (carbon) and B (oxygen). Their distribution positions occupied the entire part, demonstrating the identical spreading of these two elements.

XRD patterns of the c-MWCNT (a), TiN (b) and c-MWCNT/TiN nanocomposite (c) are revealed in Fig. 2a. The c-MWCNT (a) displayed the characteristic peaks at  $26^\circ$  respect to the (001) plane of c-MWCNT. In the XRD pattern of TiN, the characteristic diffraction peaks are observed at  $37.1, 43.1, 62.5, 75.1,$  and  $79.0^\circ$  which are indexed with (111), (200), (220), (311), and (222) crystal planes of the face-centered cubic structure (fcc) of TiN (JCPDS No. 01–087–0633), respectively. The XRD pattern of c-MWCNT/TiN nanocomposite (c) presented with all the aforesaid characteristic peaks of c-MWCNT and TiN, endorses the formation of c-MWCNT/TiN nanocomposite. Figure 2b represents the Raman spectrum of c-MWCNT (a) and c-MWCNT/TiN nanocomposite (b). The c-MWCNT (a) showed D and G bands at  $1358$  and  $1603\text{ cm}^{-1}$ , respectively. The D band is usually related to the lattice distortion or defect of carbon, and the G band represents the  $sp^2$  hybridized carbon atoms [24]. In the case of c-MWCNT/TiN nanocomposite (b), the bands at  $258, 406,$  and  $609\text{ cm}^{-1}$  represented the Raman scattering of TiN. The bands at  $258$  and  $406\text{ cm}^{-1}$  were ascribed to acoustical phonons, and those at  $609\text{ cm}^{-1}$  were attributed to

**Fig. 1** TEM image (a & b), and elemental mapping (c-titanium, d-nitrogen) of c-MWCNT/TiN

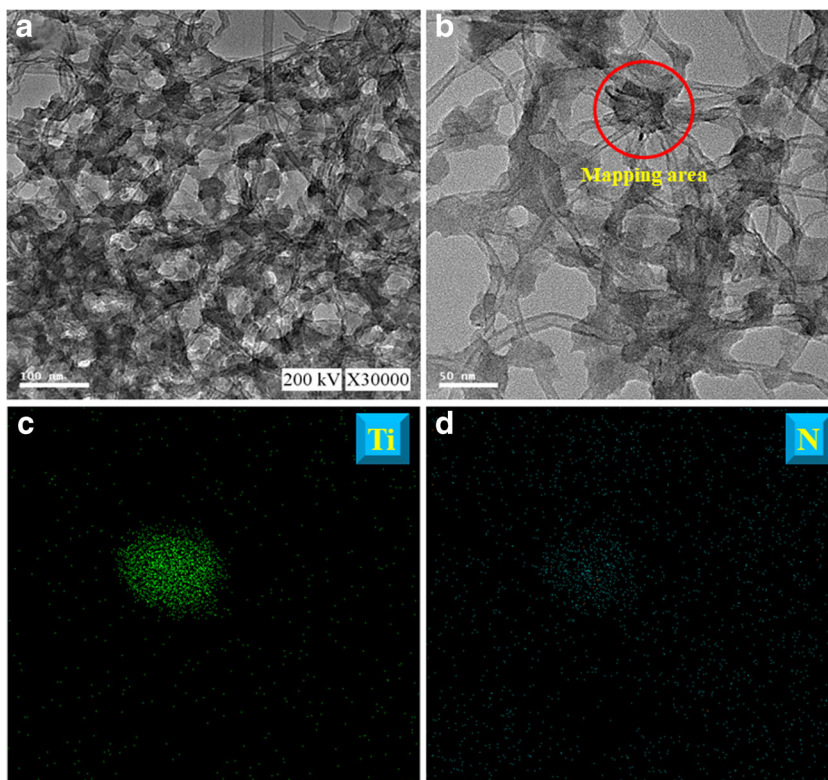
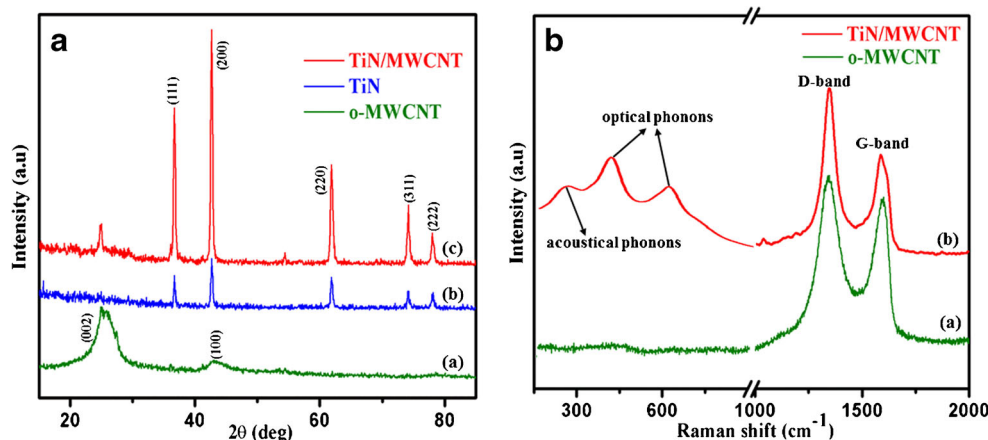


**Fig. 2** a.) XRD spectra of c-MWCNT (a), TiN (b), and c-MWCNT/TiN (c). b.) Raman spectra of c-MWCNT (a), and c-MWCNT/TiN (b)



optical phonons [25]. The spectrum of c-MWCNT/TiN nanocomposite (b) also reveals two bands located at about 1358 and 1603  $\text{cm}^{-1}$  that can be due to the presence of c-MWCNT. Besides, the  $I_D/I_G$  ratio of c-MWCNT/TiN nanocomposite (b) is higher than the c-MWCNT (a), indicating that the decoration of TiN nanoparticles rapidly increasing the defect sites on c-MWCNT/TiN nanocomposite. These defect sites can accelerate the electrochemical conductivity of the final nanocomposite. Further, these analyses confirmed the successful formation of the c-MWCNT/TiN nanocomposite.

### Electrochemical impedance spectra (EIS) and active surface area calculation

Fig. S2A displays the Nyquist plots (impedance curve) of bare GCE (a), TiN/GCE (b), c-MWCNT/GCE (c), and c-MWCNT/TiN/GCE (d) in 1 mM  $[\text{Fe}(\text{CN})_6]^{3-/4-}$  (redox probe) containing 0.1 M KCl. In Nyquist plots, the diameter of the semicircle is the charge transfer resistance ( $R_{ct}$ ) of the modified electrode for the redox probe. The calculated  $R_{ct}$  value of TiN/GCE (175  $\Omega$ ) is higher than the bare GCE (95  $\Omega$ ), ascribed to the semiconducting property of TiN which decrease the electron transfer between electrode and electroactive redox probe. It can be found on the c-MWCNT/GCE (13  $\Omega$ ) the  $R_{ct}$  value is smaller than the bare GCE, indicating the excellent electron transfer ability of c-MWCNT. Interestingly, c-MWCNT/TiN/GCE modified electrode (7  $\Omega$ ) exhibited a significantly reduced interface electron impedance than the other modified and bare electrodes, signifying that combining of TiN with c-MWCNT can dramatically enhance the interfacial electron transfer rate among the modified electrode and redox species, due to the improved ionic conductivity and electrocatalytic activity, and the synergistic effect of c-MWCNT/TiN nanocomposite.

CVs were performed at bare GCE, TiN/GCE, c-MWCNT/GCE and c-MWCNT/TiN/GCE in 0.1 M KCl solution containing 1 mM  $[\text{Fe}(\text{CN})_6]^{3-/4-}$  at a scan rate of 50  $\text{mV s}^{-1}$  see in Fig. S2B. A quasi reversible one-electron redox peak of

$[\text{Fe}(\text{CN})_6]^{3-/4-}$  were observed for all the four electrodes. The peak separations towards  $[\text{Fe}(\text{CN})_6]^{3-/4-}$  at various electrodes drop in the order c-MWCNT/TiN/GCE ( $\Delta E_p = 94$  mV) < c-MWCNT/GCE ( $\Delta E_p = 96$  mV) < bare GCE ( $\Delta E_p = 99$  mV) < TiN/GCE ( $\Delta E_p = 220$  mV). TiN/GCE showed a higher  $\Delta E_p$  value than the bare GCE, attributed to the semiconducting property of TiN. After being modified with c-MWCNT/TiN, the peak current was increased and a lower  $\Delta E_p$  value were received, indicating c-MWCNT/TiN nanocomposite holds excellent electron transfer capability with newer functionalities than that of c-MWCNT/GCE and TiN/GCE.

The electroactive surface area of c-MWCNT/TiN/GCE was evaluated by using the Randles–Sevcik Eq. (1) [26]. Thus, the scan rate studies were performed in  $[\text{Fe}(\text{CN})_6]^{3-/4-}$  by changing the scan rates from 20 to 200  $\text{mV s}^{-1}$  (Fig. S2C).

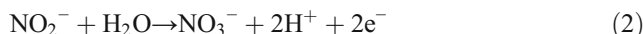
$$I_p = 2.69 \times 10^5 n^{3/2} AD^{1/2} C \nu^{1/2} \quad (1)$$

where D is the diffusion coefficient of  $[\text{Fe}(\text{CN})_6]^{3-/4-}$  ( $\text{cm}^2 \text{ s}^{-1}$ ),  $I_p$  is the anodic or cathodic peak current (A), C is the concentration of the  $[\text{Fe}(\text{CN})_6]^{3-/4-}$  ( $\text{mol cm}^{-3}$ ), A is the electroactive area ( $\text{cm}^2$ ), n is the number of transferred electrons and  $\nu^{1/2}$  is the square root of scan rate ( $\text{mV s}^{-1}$ ). For the calculations, we have selected the slope of  $I_{pa}$  vs  $\nu^{1/2}$  (Fig. S2D). The calculated electrochemical active surface areas are 0.071, 0.083, 0.095, and 0.112  $\text{cm}^2$  for the bare GCE, TiN/GCE, c-MWCNT/GCE and c-MWCNT/TiN/GCE, respectively. The large electroactive surface of c-MWCNT/TiN nanocomposite modified electrode can furnish a better electrochemical sensing performance. The combination of c-MWCNT and TiN exhibits a large specific surface area and low charge transfer resistance, therefore c-MWCNT/TiN/GCE might possess the better electrocatalytic property than the other modified electrodes.

## Electrochemical behavior of c-MWCNT/TiN at different modified electrodes

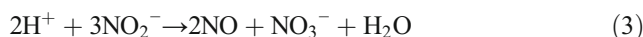
The electrochemical performance for the oxidation of nitrite at various modified electrodes was investigated by CV in 0.05 M phosphate buffer (pH 7) at a scan rate of  $50 \text{ mV s}^{-1}$ , shown in Fig. 3a. The bare GCE (a) showed a broad anodic oxidation peak for  $200 \mu\text{M}$  nitrite at a peak potential of  $0.98 \text{ V}$  ( $E_{pa}$ ) with a current response of  $9.44 \mu\text{A}$  ( $I_{pa}$ ). For the TiN/GCE (b) and c-MWCNT/GCE (c), the oxidation peak potential appeared at  $0.84$  and  $0.81 \text{ V}$ , respectively, with a substantially improvement in current response ( $I_{pa}$ ) than that of bare electrode. Interestingly, the c-MWCNT/TiN/GCE (d) exhibits a sharp, well-defined anodic peak with a significant reduction in over potential ( $0.8 \text{ V}$ ) compared with other electrodes. The received current response ( $I_{pa}$ ) for nitrite oxidation at c-MWCNT/TiN/GCE (d) is  $64.3 \mu\text{A}$ , which is 6.8-fold, 1.7-fold, 1.5-fold higher than the current response at bare GCE (a), TiN/GCE (b), and c-MWCNT/GCE, respectively. This indicates that the c-MWCNT/TiN nanocomposite effectively electrooxidizes the nitrite at the electrode surface. The excellent electrocatalytic activity of c-MWCNT/TiN/GCE attributed to the factor: upon introducing TiN nanoparticles on c-MWCNT, the conductivity and surface area of the composite has improved than the pristine c-MWCNT and TiN, leads to rapid electron transfer rate between analyte and modified

electrode. Additionally, the synergetic effect of c-MWCNT and TiN can enhance the nitrite oxidation at c-MWCNT/TiN/GCE. The oxidation reaction of nitrite proceeds via two electrons transfer from  $\text{NO}_2^-$  to form  $\text{NO}_3^-$ , the probable mechanism of nitrite oxidation can be written as given below [27],



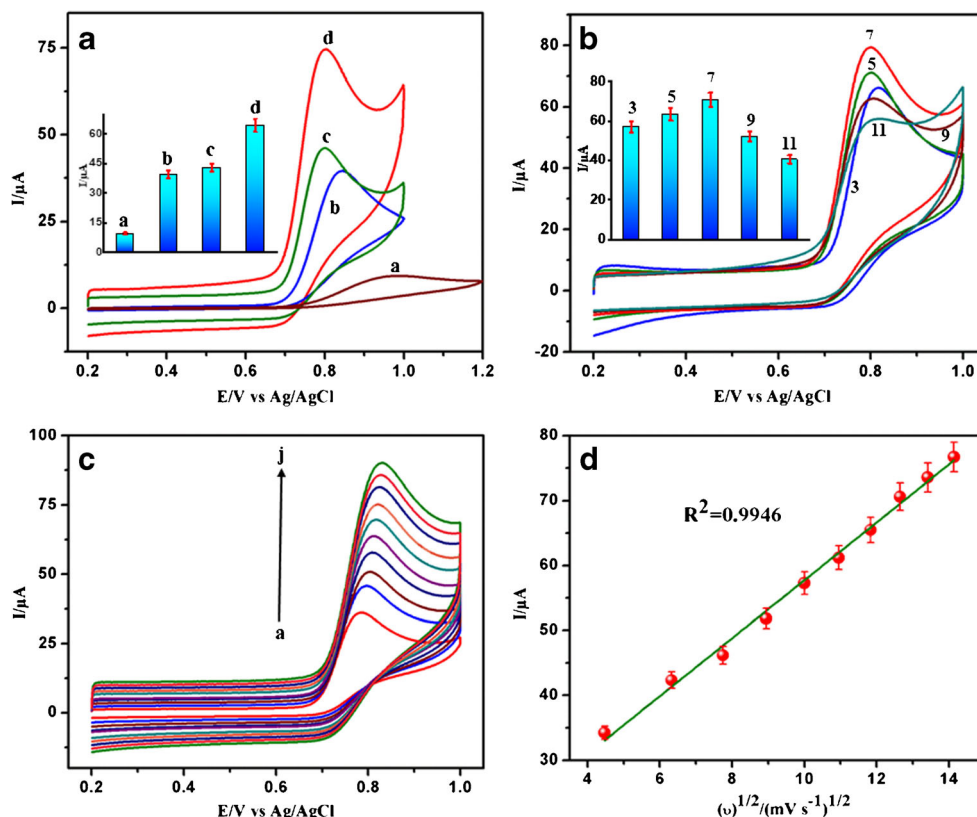
### Influence of pH and scan rate

To understand the influence of pH on the electrocatalytic activity of c-MWCNT/TiN/GCE towards the oxidation of nitrite, CVs were performed in the pH range from 3 to 11 with  $200 \mu\text{M}$  nitrite at a scan rate of  $50 \text{ mV s}^{-1}$ . As depicted in Fig. 3b, the anodic peak current of nitrite oxidation is increased while increase in the pH range of 3 to 7 and then adversely decreased beyond pH 7. Normally, nitrite is unstable in strong acidic medium, due to the conversion of nitrite into NO and  $\text{NO}_3^-$  [28], as follows,



From this, the nitrite oxidation on the catalytic sites is more preferred at neutral pH. The maximum peak current response was observed at pH 7. The nitrite oxidation is more difficult in

**Fig. 3** a.) CVs for  $200 \mu\text{M}$  nitrite in pH 7 (phosphate buffer) at a scan rate of  $50 \text{ mV s}^{-1}$  using bare GCE (a), TiN/GCE (b), c-MWCNT/GCE (c), and c-MWCNT/TiN/GCE (d) (inset: bar graph of current response of difference electrodes ( $n = 3$ )). b.) CVs for  $200 \mu\text{M}$  nitrite in various pH (3,5,7,9, and 11) (phosphate buffer) at a scan rate of  $50 \text{ mV s}^{-1}$  using c-MWCNT/TiN/GCE (inset: bar graph of current response at different pH ( $n = 3$ )). c.) Current response of c-MWCNT/TiN/GCE for  $200 \mu\text{M}$  nitrite in buffer (pH 7) with various scan rates 20, 40, 60, 80, 100, 120, 140, 160, 180, and  $200 \text{ mV s}^{-1}$  (a-j). d.) plot between the square root of the scan rate ( $v^{1/2}$ ) and current response ( $I_{pa}$ ) ( $n = 3$ )



basic medium, which is due to the proton deficiency [29]. Therefore, while increasing the pH beyond 7, the anodic current of nitrite oxidation is conversely decreased. Hence, pH 7 was selected as an optimum electrolyte for nitrite detection.

To investigate the kinetics of the electrochemical oxidation, CVs were performed for the anodic oxidation of 200  $\mu\text{M}$  nitrite on c-MWCNT/TiN/GCE at various scan rates from 20 to 200  $\text{mV s}^{-1}$  in pH 7 buffer. From Fig. 3c the anodic peak current ( $I_{pa}$ ) was increased and the oxidation peak potential ( $E_{pa}$ ) was shifted to more positive side. As can be seen from Fig. 3d, the anodic peak current ( $I_{pa}$ ) had a good linear relationship with the square root of the scan rate ( $\nu^{1/2}$ ), the corresponding correlation coefficient ( $R^2$ ) to be 0.9946. The result clearly suggests that the kinetics of the nitrite oxidation on c-MWCNT/TiN/GCE is diffusion-controlled electron transfer process [30]. For a totally irreversible diffusion-controlled process, the number of electrons ( $n$ ) involved in the overall oxidation of nitrite is calculated from the slope of  $I_{pa}$  vs  $\nu^{1/2}$  plot (Fig. 3d) using the Eq. (4) given below [31].

$$I_p = 2.99 \times 10^5 n[(1-\alpha) n_\alpha]^{1/2} C_0 D^{1/2} A \nu^{1/2} \quad (4)$$

where,  $C_0$  is nitrite concentration ( $\text{mol cm}^{-3}$ ),  $D$  is diffusion coefficient of nitrite ( $3.7 \times 10^{-5} \text{ cm}^2 \text{ s}^{-1}$ ) [32],  $A$  is electrode area. By applying this values in Eq. (4), the calculated value of  $n$  was found to be 1.79, validates that the oxidation of nitrite on c-MWCNT/TiN/GCE is a two-electron transfer process.

To understand the fast electron transfer reaction of nitrite ion at c-MWCNT/TiN/GCE, the standard heterogeneous rate constant ( $k_s$ ) for nitrite at bare GCE, TiN/GCE, c-MWCNT/GCE and c-MWCNT/TiN/GCE was calculated by using Velasco Eq. (4) [33].

$$k_s = 1.11 D_0^{1/2} (E_p - E_{p/2})^{-1/2} \nu^{1/2} \quad (5)$$

where,  $k_s$  is standard heterogeneous constant,  $D_0$  is the apparent diffusion coefficient ( $3.7 \times 10^{-5} \text{ cm}^2 \text{ s}^{-1}$ ) [32],  $E_p$  is oxidation peak potential,  $E_{p/2}$  is half-wave oxidation peak potential and  $\nu$  is the scan rate. For the bare GCE, TiN/GCE, c-MWCNT/GCE and c-MWCNT/TiN/GCE, the estimated heterogeneous rate constant ( $k_s$ ) for the oxidation of nitrite ion were found to be  $1.89 \times 10^{-3}$ ,  $4.09 \times 10^{-3}$ ,  $6.23 \times 10^{-3}$  and  $1.26 \times 10^{-2} \text{ cm s}^{-1}$ , respectively. The higher  $k_s$  value at c-MWCNT/TiN/GCE suggests that the oxidation of nitrite is much faster than at the c-MWCNT/GCE, TiN/GCE and bare GCE.

### Amperometric determination of nitrite

Amperometry was utilized to determine the nitrite at c-MWCNT/TiN modified electrode. As shown in Fig. 4a, amperometric i-t response of nitrite in phosphate buffer (pH

7) was acquired at the standard potential +0.8 V (1400 rpm) upon the consecutive addition of nitrite. The nitrite concentration was altered every 50s with continuous stirring by rotating disk electrode (RDE). The obtained response current was stable within 4 s. The oxidation i-t response current in direct relationship to the nitrite concentrations in the wide range of 6 nM to 950  $\mu\text{M}$ , revealed in Fig. 4b. The corresponding linear regression equation with the correlation coefficient can be written as following,

$$I_{pa}(\mu\text{N}) = 0.709 [\text{Nit}] (\mu\text{M}) + 4.8908; R^2 = 0.9955 \quad (6)$$

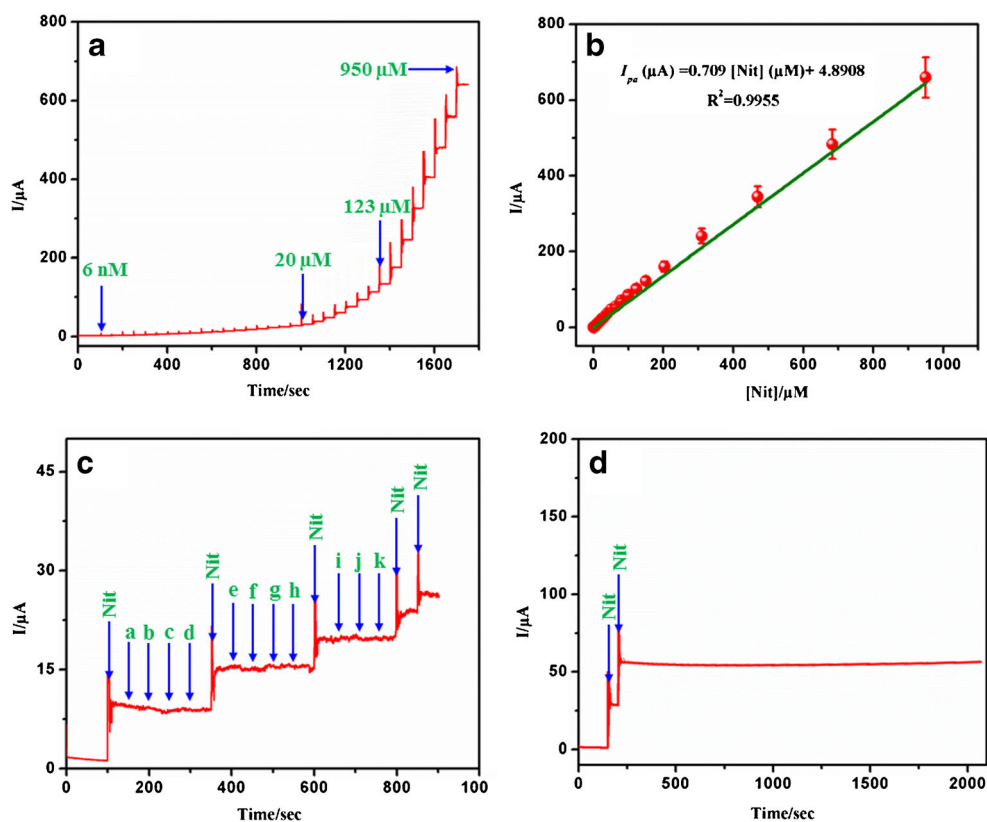
The limit of detection (LOD) =  $3(S_a/b)$ , where  $S_a$  represents the standard deviation of intercept,  $b$  is the slope of the calibration plot [34], using these values the calculated LOD is 4 nM. The calculated sensitivity of the sensor to be  $6.63 \mu\text{A } \mu\text{M}^{-1} \text{ cm}^{-2}$ . The electrocatalytic sensing performance of c-MWCNT/TiN/RDE was compared with various modified electrodes for the determination of nitrite see Table 1. These results confirm that the sensor showed the excellent electrocatalytic performance in terms of broad working range and the better LOD than the previously reported methods.

Ag– silver nanoparticles; P(MMA-co-AMPS)– copolymer of methyl methacrylate (MMA) and 2-acrylamido-2-methylpropane sulfonic acid; PDDA– Poly (diallyldimethylammonium chloride); rGO– reduced graphene oxide; CoL– sodium [N,N'-bis(5-sulfosalicyliden)-4-chloro-1,2-phenylendiimino] cobaltate(II); MNSs– magnetite nanospheres; CPE– carbon paste electrode; Pd– palladium nanoparticles; SWCNT– single walled carbon nanotube; AgMCs-PAA/PVA–silver microcubics-polyacrylic acid/poly vinyl alcohol; SPCE– screen printed carbon electrode; CQDs– Carbon quantum dots; PEDOT– Poly(3,4-ethylenedioxythiophene);

### Selectivity, stability and reproducibility

The selectivity of the sensor is vital for finding further access to practical application, because some possible interfering compounds may interfere with c-MWCNT/TiN modified electrode for the detection of nitrite. Subsequently, we have studied the selectivity of the sensor for the determination of nitrite by addition of interfering substances into the buffer (pH 7) with the 50  $\mu\text{M}$  nitrite using amperometry. The results are depicted in Fig. 4c, which demonstrated the influence of the possibly interfering ions (a)  $\text{SO}_3^-$ , (b)  $\text{NO}_3^-$ , (c)  $\text{BrO}_3^-$ , (d)  $\text{ClO}_3^-$ , (e)  $\text{Pb}^{2+}$ , (f)  $\text{Cu}^{2+}$ , (g)  $\text{Hg}^{2+}$ , (h)  $\text{Cd}^{2+}$ , (i)  $\text{IO}_3^-$ , (j)  $\text{SCN}^-$ , (k)  $\text{CO}_3^{2-}$  in 10-fold excess. From this result, it can be clearly seen that obvious changes in current response when nitrite was added and quickly reached a stable value. Addition of the above-mentioned interfering substances, does not interfere with the current response of nitrite detection, however the

**Fig. 4** a.) Amperometric current response for c-MWCNT/TiN/RDE in pH 7 buffer containing various concentration of nitrite from 6 nM to 950  $\mu$ M (applied potential = +0.8 V). b.) Calibration plot of response current vs the concentrations of nitrite ( $n = 3$ ). c.) Current response for various species including (a)  $\text{SO}_3^-$ , (b)  $\text{NO}_3^-$ , (c)  $\text{BrO}_3^-$ , (d)  $\text{ClO}_3^-$ , (e)  $\text{Pb}^{2+}$ , (f)  $\text{Cu}^{2+}$ , (g)  $\text{Hg}^{2+}$ , (h)  $\text{Cd}^{2+}$ , (i)  $\text{IO}_3^-$ , (j)  $\text{SCN}^-$ , (k)  $\text{CO}_3^{2-}$  in the presence of nitrite. d.) Operational stability curve of c-MWCNT/TiN/RDE



presence of these ions the activity of the sensor is insignificantly decreased. These results proved that the c-MWCNT/TiN modified electrode had a good selectivity towards the nitrite detection even in the presence of various interfering compounds.

The stability of the c-MWCNT/TiN modified electrode was verified with 200  $\mu$ M nitrite through 2000 s time period, see Fig. 4d. This result proved that the current response of nitrite at c-MWCNT/TiN modified electrode did not notably decrease up to 2000 s and 95.6% of current was retained from its original current value. So as to know the reproducibility of

the c-MWCNT/TiN modified electrode, five different electrodes were separately used to measure the current response towards 200  $\mu$ M nitrite with the relative standard deviation (% RSD) being 2.1%. These results clearly confirm that our modified electrode is highly stable and has an appreciable reproducibility.

### Determination of nitrite in real water samples

Practical applicability of c-MWCNT/TiN modified electrode was verified in various real samples. Real samples such as

**Table 1** Comparison of electrocatalytic performance of c-MWCNT/TiN/RDE for nitrite determination with previously reported methods

Electrode	$E_{pa}$ (V)	Linear range ( $\mu$ M)	LOD (nM)	Ref
Ag-P(MMA-co-AMPS)/GCE	0.9	1.0–100,000	200	[3]
PDDA-rGO/GCE	0.75	0.5–2000	200	[8]
CoL/MNSs/CPE	1.0	0.2–30.0	15	[9]
$\text{Co}_3\text{O}_4$ /rGO/GCE	–	1–380	140	[10]
Au-Pd/rGO/GCE	0.85	0.05–1000	20	[28]
Pd/SWCNT/GCE	1.0	2–238	250	[32]
AgMCs-PAA/PVA/SPCE	–	283–1230	4500	[34]
CQD-PEDOT	0.8	0.50–1110	88	[35]
$\text{TiO}_2$ /hemin/GCE	0.75	0.6–133	59	[36]
c-MWCNT/TiN/GCE	0.8	0.006–950	4	This work

pond, river, packaged water and meat samples were collected from pond aquarium, Xindian River, and local market, respectively. Before the experiments, as collected water samples were filtered with a 0.45  $\mu\text{m}$  filter paper to remove the suspended matters. The extraction of nitrite ions from the meat samples was accomplished by leaving a certain amount of crushed sample in deionized water at 70  $^{\circ}\text{C}$  under stirring for 10 min and then filtering the remaining liquid. When the native water samples were analyzed, no current response corresponding to nitrite was detected. Following to this, the determination nitrite in spiked samples of water and meat samples was performed with three various concentrations of nitrite, the results are summarized in Table S1.

## Conclusion

A novel, efficient electrochemical sensor was successfully developed for the detection of nitrite, c-MWCNT/TiN was used as an electrode modifier. Due the excellent synergistic effect of c-MWCNT and TiN, a large surface area, low electrochemical resistivity ( $R_{\text{ct}} = 7 \Omega$ ), enhanced electroactive surface ( $A = 0.112 \text{ cm}^2$ ) and higher heterogeneous electron transfer rate ( $k_s = 1.26 \times 10^{-2} \text{ cm s}^{-1}$ ) was achieved at c-MWCNT/TiN/GCE. Under optimized condition, the c-MWCNT/TiN modified electrode can selectively detect the nitrite in the range from 6 nM to 950  $\mu\text{M}$  with a limit of detection of 4 nM. The sensor showed a good selectivity, high stability and reproducibility. The real time viability of the sensor was confirmed by determination of nitrite in real water and meat samples with good recoveries.

**Acknowledgements** The authors gratefully acknowledge the financial support of the Ministry of Science and Technology, Taiwan through contract no. MOST 107-2113-M-027-005-MY3.

**Compliance with ethical standards** The author(s) declare that they have no competing interests.

**Publisher's Note** Springer Nature remains neutral with regard to jurisdictional claims in published maps and institutional affiliations.

## References

- Jasman SM, Lintang HO, Yuliati L (2017) Enhanced detection of nitrite ions over copper acetylacetonate/polymeric carbon nitride composites. *Macromol Symp* 371:84–93
- Gómez J, Sanjuán N, Bon J, Arnau J, Clemente G (2015) Effect of temperature on nitrite and water diffusion in pork meat. *J Food Eng* 149:188–194
- Rastogi PK, Ganesan V, Krishnamoorthi S (2014) A promising electrochemical sensing platform based on a silver nanoparticle decorated copolymer for sensitive nitrite determination. *J Mater Chem A* 2:933–943
- He C, Howes BD, Smulevich G, Rumpel S, Reijerse EJ, Lubitz W, Cox N, Knipp M (2015) Nitrite dismutase reaction mechanism: kinetic and spectroscopic investigation of the interaction between nitrophorin and nitrite. *J Am Chem Soc* 137:4141–4150
- Farhadinejad T, Khakzad A, Jafari M, Shoaee Z, Khosrotehrani K, Nobari R, Shahrokhi V (2014) The study of environmental effects of chemical fertilizers and domestic sewage on water quality of Taft region, Central Iran. *Arab J Geosci* 7:221–229
- Huang YG, Ji JD, Hou QN (1996) A study on carcinogenesis of endogenous nitrite and nitrosamine, and prevention of cancer. *Mutat Res Fundam Mol Mech Mutagen* 358:7–14
- Moorcroft MJ, Davis J, Compton RG (2001) Detection and determination of nitrate and nitrite: a review. *Talanta* 54:785–803
- Xu F, Deng M, Liu Y, Ling X, Deng X, Wang L (2014) Facile preparation of poly (diallyldimethylammonium chloride) modified reduced graphene oxide for sensitive detection of nitrite. *Electrochem Commun* 47:33–36
- Parsaei M, Asadi Z, Khodadoust S (2015) A sensitive electrochemical sensor for rapid and selective determination of nitrite ion in water samples using modified carbon paste electrode with a newly synthesized cobalt (II)-Schiff base complex and magnetite nanospheres. *Sensors Actuators B Chem* 220:1131–1138
- Haldorai Y, Kim JY, Vilian ATE, Heo NS, Huh YS, Han YK (2016) An enzyme-free electrochemical sensor based on reduced graphene oxide/Co<sub>3</sub>O<sub>4</sub> nanospindle composite for sensitive detection of nitrite. *Sensors Actuators B Chem* 227:92–99
- Newbery JE, Haddad MPL (1985) Amperometric determination of nitrite by oxidation at a glassy carbon electrode. *Analyst* 110:81–82
- Moon JM, Thapliyal N, Hussain KK, Goyal RN, Shim YB (2018) Conducting polymer-based electrochemical biosensors for neurotransmitters: a review. *Biosens Bioelectron* 102:540–552
- Cai H, Cao X, Jiang Y, He P, Fang Y (2003) Carbon nanotube-enhanced electrochemical DNA biosensor for DNA hybridization detection. *Anal Bioanal Chem* 375:287–293
- Erdem A, Papakonstantinou P, Murphy H (2006) Direct DNA hybridization at disposable graphite electrodes modified with carbon nanotubes. *Anal Chem* 78:6656–6659
- Sinha A, Jain R, Zhao H, Karolia P, Jadon N (2018) Voltammetric sensing based on the use of advanced carbonaceous nanomaterials: a review. *Microchim Acta* 185:89. <https://doi.org/10.1007/s00604-017-2626-0>
- Wang W, Xie Y, Xia C, Du H, Tian F (2014) Titanium dioxide nanotube arrays modified with a nanocomposite of silver nanoparticles and reduced graphene oxide for electrochemical sensing. *Microchim Acta* 181:1325–1331
- Xie Y, Meng Y (2014) SERS performance of graphene oxide decorated silver nanoparticle/titania nanotube array. *RSC Adv* 4:41734–41743
- Avasarala B, Haldar P (2010) Electrochemical oxidation behavior of titanium nitride based electrocatalysts under PEM fuel cell conditions. *Electrochim Acta* 55:9024–9034
- Li CT, Li SR, Chang LY, Lee CP, Chen PY, Sun SS, Lin JJ, Vittal R, Ho KC (2015) Efficient titanium nitride/titanium oxide composite photoanodes for dye-sensitized solar cells and water splitting. *J Mater Chem A* 3:4695–4705
- Fischer A, Makowski P, Muller JO, Antonietti M, Thomas A, Goettmann F (2008) High-surface-area TiO<sub>2</sub> and TiN as catalysts for the C–C coupling of alcohols and ketones. *ChemSusChem* 1:444–449
- Xie Y, Wang Y, Du H (2013) Electrochemical capacitance performance of titanium nitride nanoarray. *Mater Sci Eng B* 178:1443–1451
- Lu XH, Wang GM, Zhai T, Yu MH, Xie SL, Ling YC, Liang CL, Tong YX, Li Y (2012) Stabilized TiN nanowire arrays for high-performance and flexible supercapacitors. *Nano Lett* 12:5376–5381



23. Xie Y, Song F, Du H, Xia C (2015) Preparation of carbon-coated lithium iron phosphate/titanium nitride for a lithium-ion supercapacitor. *New J Chem* 39:604–613
24. Balasubramanian P, Balamurugan TST, Chen SM, Chen TW, Tseng TW, Lou BS (2018) A simple architecture of cellulose microfibril/reduced graphene oxide nanocomposite for the electrochemical determination of nitrobenzene in sewage water. *Cellulose* 25:2381–2391
25. Sedira S, Achour S, Avci A, Eskizeybek V (2014) Physical deposition of carbon doped titanium nitride film by DC magnetron sputtering for metallic implant coating use. *Appl Surf Sci* 295:81–85
26. Balasubramanian P, Settu R, Chen SM, Chen TW (2018) Voltammetric sensing of sulfamethoxazole using a glassy carbon electrode modified with a graphitic carbon nitride and zinc oxide nanocomposite. *Microchim Acta* 185:396
27. Zhang J, Chen Z, Wu H, Wu F, He C, Wang B, Wu Y, Ren Z (2016) An electrochemical bifunctional sensor for the detection of nitrite and hydrogen peroxide based on layer-by-layer multilayer films of cationic phthalocyanine cobalt (ii) and carbon nanotubes. *J Mater Chem B* 4:1310–1317
28. Li SS, Hu YY, Wang AJ, Weng X, Chen JR, Feng JJ (2015) Simple synthesis of worm-like Au–Pd nanostructures supported on reduced graphene oxide for highly sensitive detection of nitrite. *Sensors Actuators B Chem* 208:468–474
29. Balasubramanian P, Balamurugan TST, Chen SM (2017) Highly sensitive electrochemical detection of nitrite ions in food samples via  $\beta$ -cyclodextrin capped gold nanoparticles film modified glassy carbon electrode. *J Electrochem Soc* 164:B715–B722
30. Balasubramanian P, Settu R, Chen SM, Chen TW, Sharmila G (2018) A new electrochemical sensor for highly sensitive and selective detection of nitrite in food samples based on sonochemical synthesized calcium ferrite ( $\text{CaFe}_2\text{O}_4$ ) clusters modified screen printed carbon electrode. *J Colloid Interface Sci* 524:417–426
31. Matemadombo F, Nyokong T (2007) Characterization of self-assembled monolayers of iron and cobalt octa alkylthio substituted phthalocyanines and their use in nitrite electrocatalytic oxidation. *Electrochim Acta* 52:6856–6864
32. Pham XH, Li CA, Han KN, Huynh-Nguyen BC, Le TH, Ko E, Kim JH, Seong GH (2014) Electrochemical detection of nitrite using urchin-like palladium nanostructures on carbon nanotube thin film electrodes. *Sensors Actuators B Chem* 193:815–822
33. Velasco JG (1997) Determination of standard rate constants for electrochemical irreversible processes from linear sweep voltammograms. *Electroanalysis* 9:880–882
34. Promsuwan K, Thavarungkul P, Kanatharana P, Limbut W (2017) Flow injection amperometric nitrite sensor based on silver microcubics-poly (acrylic acid)/poly (vinyl alcohol) modified screen printed carbon electrode. *Electrochim Acta* 232:357–369
35. Jiao M, Li Z, Li Y, Cui M, Luo X (2018) Poly(3,4-ethylenedioxythiophene) doped with engineered carbon quantum dots for enhanced amperometric detection of nitrite. *Microchim Acta* 185:249
36. Ranjani B, Kalaiyarasi J, Pavithra L, Devasena T, Pandian K, Gopinath SC (2018) Amperometric determination of nitrite using natural fibers as template for titanium dioxide nanotubes with immobilized hemin as electron transfer mediator. *Microchim Acta* 185:194